CHAPTER 4

Copper oxide nanoparticles as a mild and efficient catalyst for *N*-arylation of imidazole and aniline at room temperature.

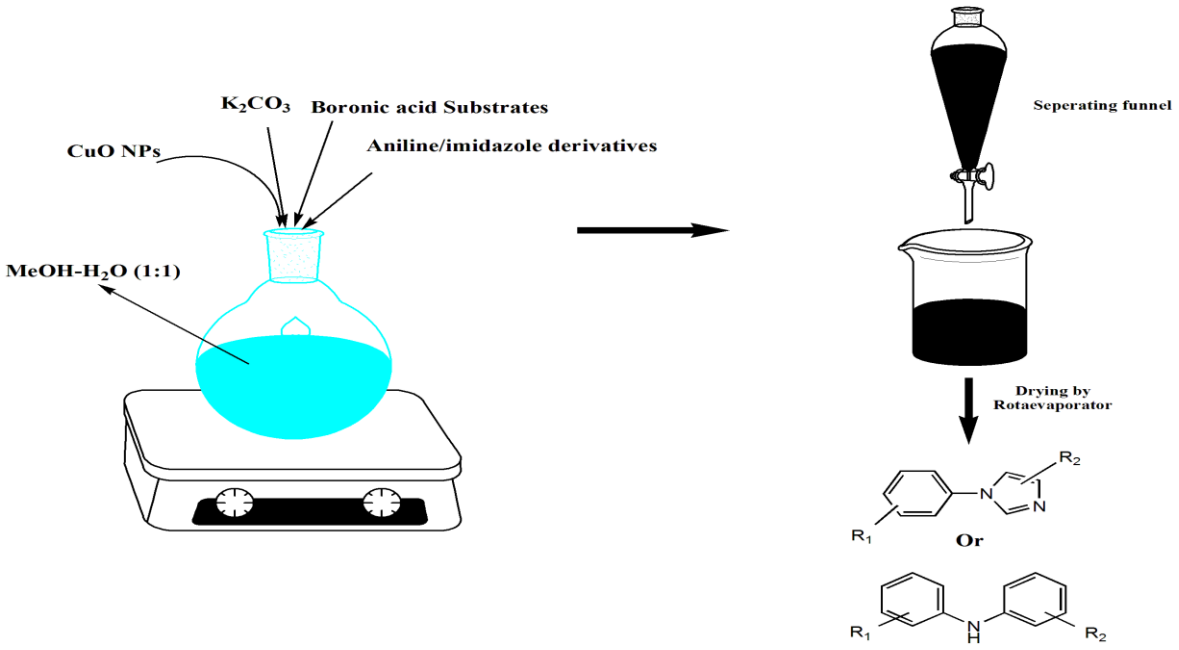

The work described in this chapter has been published in *Synlett*, 2017, 28, 1177-1182.

4.1 Introduction

In the realm of organic synthesis, transition-metal-mediated carbon-heteroatom bond forming reactions have made an immense visible contribution to the recent growth in the area. Nowadays, nitrogen containing compounds can easily be synthesized by transition-metal-catalyzed protocols which find diverse applications in the field of advanced organic synthesis. Out of them, diarylamines and *N*-arylimidazoles depict extensive interest due to their widespread presence in natural products, agrochemicals, materials, dyes, pharmaceuticals [1] and biologically active inhibitors [2].

Buchwald and Hartwig in 1999 developed individually methods for palladium catalyzed cross-coupling reaction of aryl halides and triflates with amines [3]. Though in comparison to Ullmann method [4], the process requires milder reaction conditions yet, there are some associated demerits, such as difficulties associated with aryl halides having free N-H groups [5] and the use of expensive palladium sources and ligands.

In 1998 Chan, Evan and Lam [6] developed a mild and efficient protocol for Copper mediated oxidative amination of arylboronic acid, where they used arylboronic acids as arylating agents instead of aryl halides. Arylboronic acids are organometallic compounds which have wide applicability in the modern organic synthesis owing to many advantages such as stability, structural diversity, and lower toxicity [7]. However, the method was equipped with some drawbacks like requirement of 1–2 equiv. of $Cu(OAc)_2$, large excess of arylboronic acid and long reaction time [8]. Subsequent work on the Chan–Lam coupling reaction resulted in its catalytic version [9] along with its application to other nucleophiles such as amide [10], oxime [11], sulfoximines [12] etc. for cross-coupling reaction. After that, in order to improve the efficiency of the reaction, numbers of modifications have been made using different copper salts in the presence of various ligands [10-12]. However, the reaction was generally associated with certain demerits like long reaction times and high reaction temperatures etc. and thus, further optimization is still desirable in case of this reaction.

Again nowadays, NPs are considered to be very efficient and attractive catalysts compared to their bulk counterparts, owing to their high surface to volume ratio as well as very active surface atoms. Though lots of methods are available for the synthesis of NPs [13], the routes which are based on solution-based processes are more effective for the synthesis of nanostructured materials with well controlled shapes, sizes and

structures. Amongst the metal NPs, Cu based NPs such as CuO hold a superior position because of their versatile applications in various organic syntheses like C-N bond formation reaction and C-H activation reaction and also due to their stability and easy synthesis [14]. A numbers of techniques are available in the literature related to the synthesis of CuO NPs which are generally costly, time consuming and require large volumes of reagents [15]. Consequently, a mild and simple technique for the synthesis of CuO NPs is an essentially a burning topic among researchers. Working on this direction in this chapter, we present a very efficient technique for the synthesis of CuO NPs and the resulting catalysts were successfully applied in a mild reaction protocol for *N*-arylation of imidazoles and anilines with arylboronic acids at room temperature (Scheme 1).

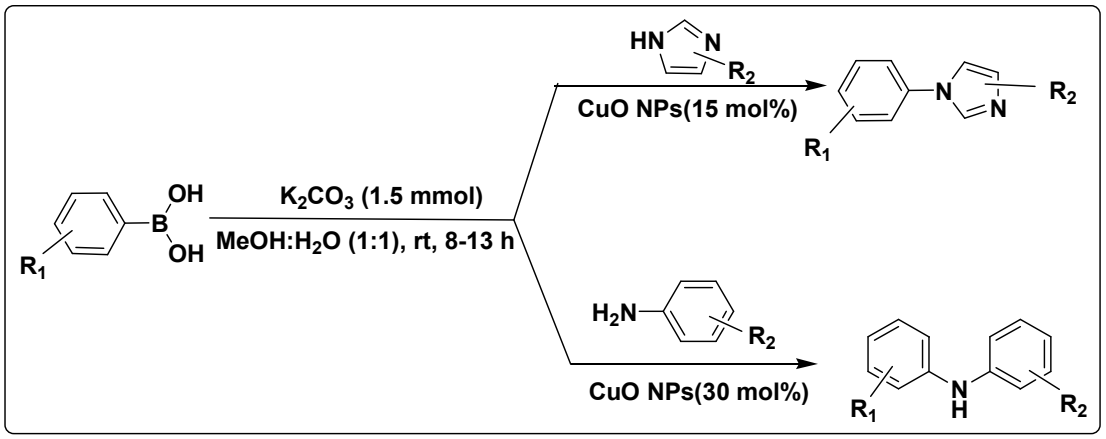

Scheme 1: *N*-Arylation of imidazoles and anilines with arylboronic acid.

Here, we have reported a simple, cost effective and eco-friendly method for the synthesis of Copper(II) oxide NPs by using copper chloride ($CuCl_2$) as the starting precursor. The as synthesized NPs were characterized using various techniques like FT-IR spectroscopy; powder XRD, SEM, EDX, TEM, TGA, XPS, BET surface area analysis and particle size analysis. The Chan-Lam coupling reaction between arylboronic acid and aniline or imidazoles substrates with different types of functional groups were assessed by using the synthesized NPs and found good to excellent yields of the desired product.

4.2. Experimental

4.2.1. General Information

The reactions were monitored by applying thin-layer-chromatography using aluminium precoated TLC plates with silica gel $60F_{254}$ (Merck) in iodine chamber. The products were purified by column chromatography technique using silica gel (60-120 mesh). ^{1}H and ^{13}C NMR spectra were recorded in a 400 MHz NMR spectrophotometer (JEOL JNM-ECS) using tetramethylsilane (TMS) as the internal standard and the coupling constants are expressed in Hertz. Melting points of the products was recorded in Büchi B450 melting point apparatus. FT-IR spectra were recorded in a Perkin Elmer FT-IR spectrophotometer (Frontier MIR-FIR). The thermogravimetric mass change of nanocatalyst was thermally characterized in Shimadzu TGA-50 instrument under static air atmosphere at 10 °C min^{-1}. The powder XRD pattern was recorded with Rigaku X-ray diffractometer over the range of 2Θ=10-80° with a scanning rate of 2 °C min^{-1}. The surface morphology and EDX analysis of CuO NPs were analyzed using SEM (JEOL, model JSM-6390 LV operating at an accelerating voltage of 15 kV). Size and distribution of NPs were determined by using TEM (JEOL, JEM-2010) equipped with a slow-scan CCD camera at an operating voltage of 200kV. The BET surface areas were determined by N_2 adsorption using a Quantachrome Instruments (Model: NOVA 1000e). XPS analysis of the catalyst was done in Industrial Chemistry & Reaction Engineering, Åbo Akademi University, 20500 Åbo-Turku, Finland.

4.2.2. Materials and chemical reagents

Chemicals were procured from different commercial firms. All the chemicals, viz. cupric chloride (Merck, India), sodium hydroxide (Merck, India), hydrochloric acid (Merck, India), capping agent (Polyethylene glycol, MW 4000, SRL India), potassium carbonate (Qualigens, India), MeOH (Merck, India), ethanol (Bengal chemicals Pvt. Ltd, Kolkata), arylboronic acid substrates (SRL, India), aniline and imidazole substrates (Merck, India & SRL, India) and silica gel for TLC and column chromatography (Merck, India) were of analytical grade and used without purification. Solvents used for purification (ethylacetate and hexane) were distilled prior to use.

4.2.3. Preparation of the catalyst

Copper(II) oxide NPs have been synthesized following the procedure opted by Goswami *et al.* [16] with some modifications in order to get obtain uniform smaller particles. Copper(II) chloride dihydrate (6.8 g), sodium hydroxide (3.2 g), and capping solvent (polyethylene glycol) were mixed in a 2:1:1.5 ratio with ethanol:water (200 mL 1:1, vol:vol) solvent system in a round bottom flask fitted with a reflux condenser. The mixture was then refluxed for 12 h and allowed to cool to room temperature. The mixture was again refluxed for 5 h. The dark brown precipitate was separated by centrifugation and then washed with ethanol, acetone and hot water respectively. The product was finally dried at room temperature and heated to 120 °C in a vacuum oven in the absence of air and allowed to cool to normal temperature, and kept in a vacuum desiccator. The catalyst was used in the *N*-arylation reactions.

4.2.3. Typical procedure for *N*-arylation of aniline with phenylboronic acid using the Cu(II)O NPs

To a 50 mL round-bottomed flask, 0.5 mmol of aniline, 1.5 mmol of boronic acid substrate, 1.5 mmol of base potassium carbonate and 30 mol% of CuO NPs with respect to aniline substrate were added and stirred in methanol:water (1:1) solvent system under air at room temperature for the required time. The monitoring of the reaction was done by TLC technique. After completion, the reaction mixture was first diluted with distilled water and then distilled ethyl acetate was used to extract the product from the reaction mixture (3 times). Thereafter it was washed with brine (3 times) and then anhydrous Na_2SO_4 was used for removal of traces of water left. Finally, column chromatography technique (60-120 mesh silica gel and ethyl acetate-hexane solvent mixture) was used to purify the product.

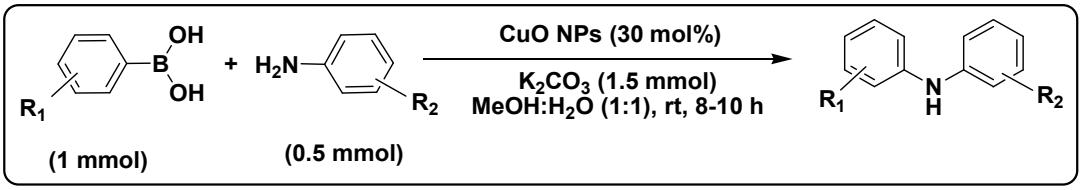

Scheme 2: Optimized reaction of *N*-arylation reaction of aniline.

4.2.4. Typical procedure for *N*-arylation of imidazole with phenylboronic acid using the Cu(II)O NPs

To a 50 mL round-bottomed flask, a mixture of 1 mmol of imidazole, 1.2 mmol of boronic acid substrate, 1.5 mmol of potassium carbonate and 15 mol% of CuO NPs with respect to imidazole substrate were added and stirred in methanol:water (1:1) solvent system under air at room temperature for the required time. The reaction was monitored by TLC. After completion of the reaction, the product was extracted with distilled ethyl acetate (3 times). The extract was washed with brine (3 times) and dried over Na_2SO_4. Finally, the product was purified using column chromatography technique (60-120 mesh silica gel, ethyl acetate-hexane solvent mixture).

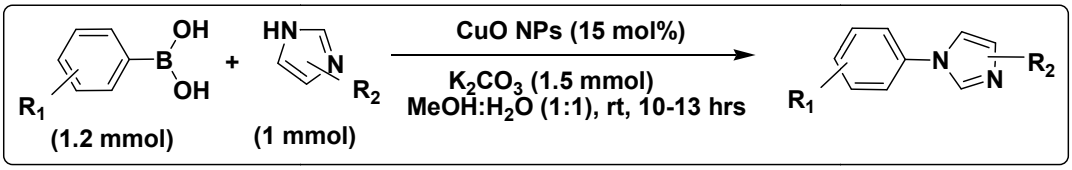

Scheme 3: Optimized reaction of *N*-arylation reaction of imidazole.

4.3. Results and Discussion

4.3.1. Characterization of CuO NPs

4.3.1.1. FT-IR spectroscopic analysis

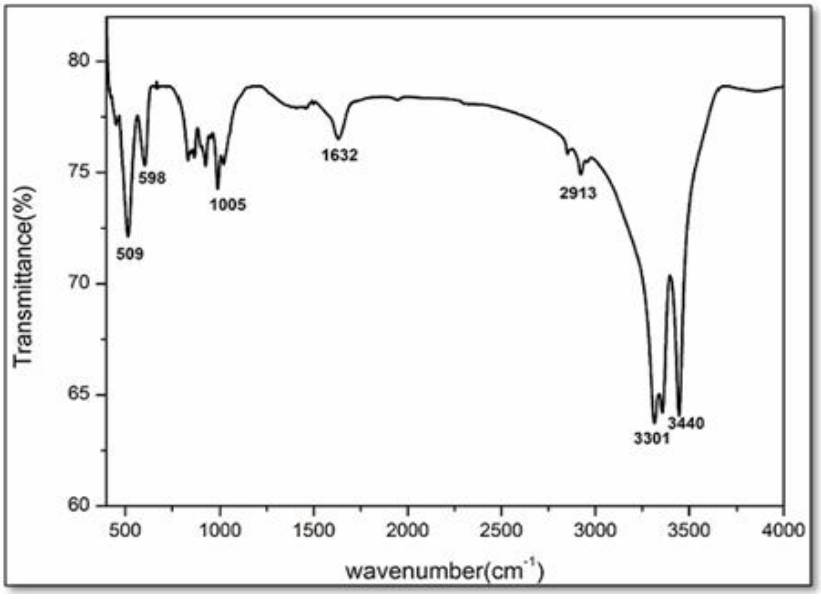

Fig. 1: FT-IR spectrum of synthesized CuO NPs.

The synthesized CuO NPs were first characterized by FT-IR spectroscopy (Fig. 1). The symmetric and asymmetric stretching of O-H bonds are observed at 2913 cm^{-1} and 3440 cm^{-1} respectively. The presence of bands at 509 cm^{-1} and 598 cm^{-1} are due to the different modes of bending vibration of the Cu-O bond [16, 17], whereas the band at 1632 cm^{-1} is assigned to C–C and C–O from residual carbonates and polymer.

4.3.1.2. Powder XRD analysis

This technique was used to determine the crystal domain size and the structure of the NPs formed. The typical XRD pattern of the synthesized CuO NPs is shown in Fig. 2. The XRD pattern (Fig. 2) indicates the presence of the various characteristic peaks which can be indexed on the basis of monoclinic CuO (JCPDS card no. 89-5895). The broadening of the XRD peak indicates that the synthesized particles are in the nano range.

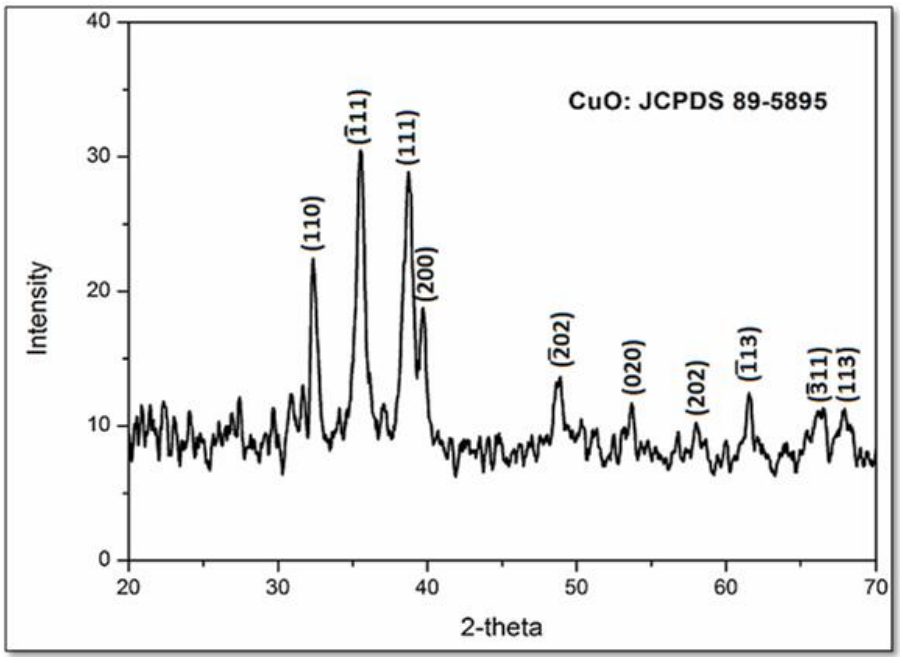

Fig. 2: PXRD pattern of CuO NPs.

4.3.1.3. SEM analysis

The SEM technique was used to determine the surface morphology of the NPs and is shown in Fig. 3 (a & b). From the SEM image, it is obvious that the particles represent needle shaped morphology. However, most of the NPs are found to be of irregular

shapes and sizes, which might be due to agglomerization of the particles.

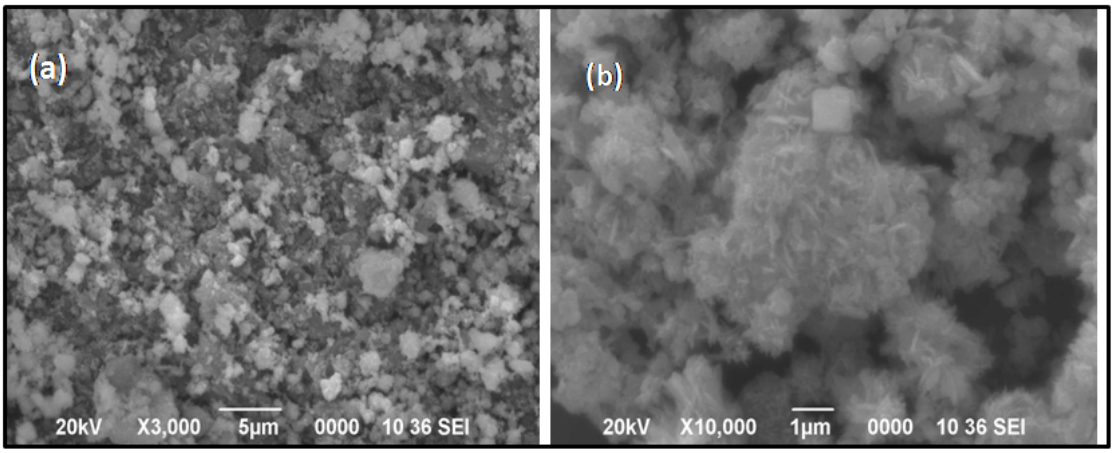

Fig. 3: SEM images of synthesized CuO NPs.

4.3.1.4. TGA analysis

The thermogravimetric analysis of CuO NPs is shown in Fig. 4. It is evident from the Fig. 4 that the nanocatalyst was thermally stable. The initial weight loss up to 100 °C might be due to elimination of physically absorbed moistures, the other weight loss up to 300 °C was due to decomposition of organic materials.

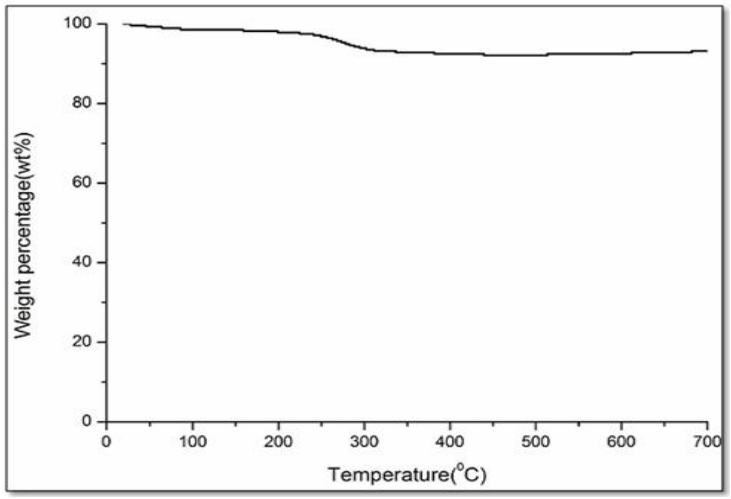

Fig. 4: TGA thermogram of CuO NPs.

4.3.1.5. BET surface area analysis

To examine the porous behaviour and to estimate the surface area of the as-prepared

CuO NPs, N_2 adsorption/desorption experiments were performed at liquid N_2 temperature (Fig. 5). The N_2 adsorption/desorption isotherm of the synthesized CuO nanostructure belongs to type IV with H1 and H3 hysteresis loop combination, a general characteristic of mesoporous materials. Also, (BET) surface area of the CuO nanostructure was found to be about 164.180 m^2g^{-1} which is much larger than that found for the commercial CuO.

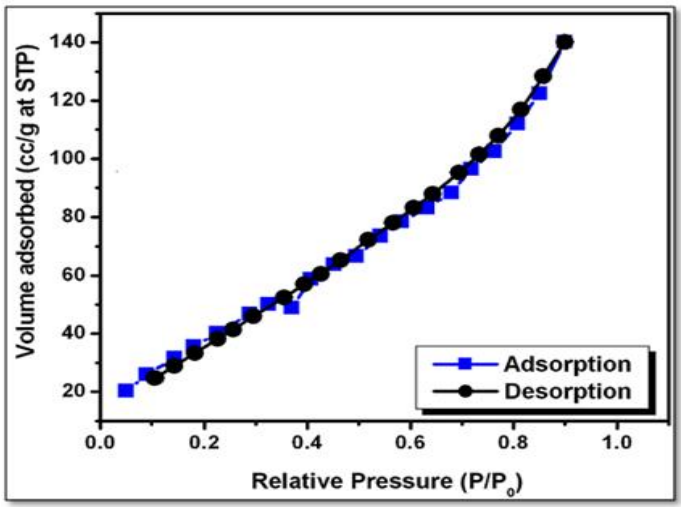

Fig. 5: N_2 adsorption/desorption of the CuO NPs.

4.3.1.6. EDX analysis of the catalyst

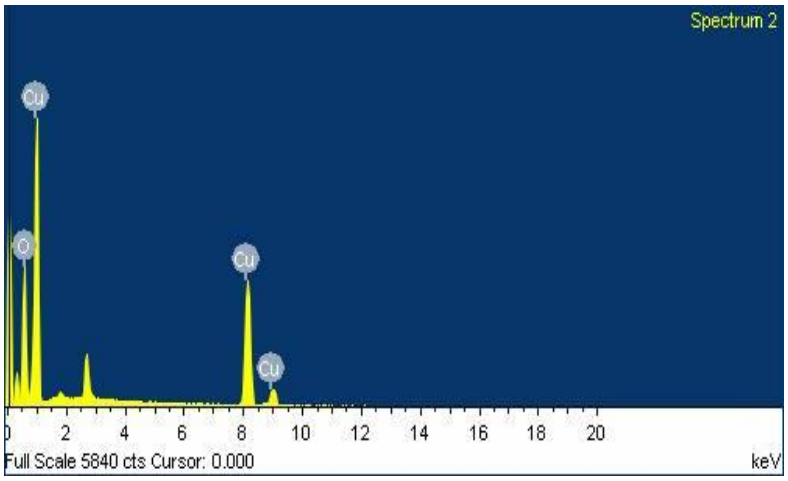

Fig. 6: EDX pattern of CuO NPs.

EDX analysis of the CuO NPs is shown in Fig.6. The EDX spectrum clearly indicates only the existence of Cu and O signals which shows the presence of Cu and O the only

element devoid of any other metal impurities.

4.3.1.7. TEM analysis

The TEM and HRTEM images of the prepared CuO NPs are presented in Fig. 7 (a & b). The TEM images show that the NPs are cylindrical in shape, the particles are few nm in range and which gets aggregated. The interplanar distance of 0.23 nm can be ascribed to the (111) plane of the monoclinic CuO. The corresponding selected area electron diffraction (SAED) pattern of the CuO NPs [inset in Fig. 7(b)] indicates that the particles are crystalline in nature and possess three well-resolved rings for (110), (-111) & (111) planes. There are also two poorly resolved rings which are for (200) and (-202) planes respectively. Fig.7(c) indicates the size distribution of the NPs which clearly shows that most of the particles fall in the range 7-17 nm size with an average particle diameter of about 12 ± 0.99 nm.

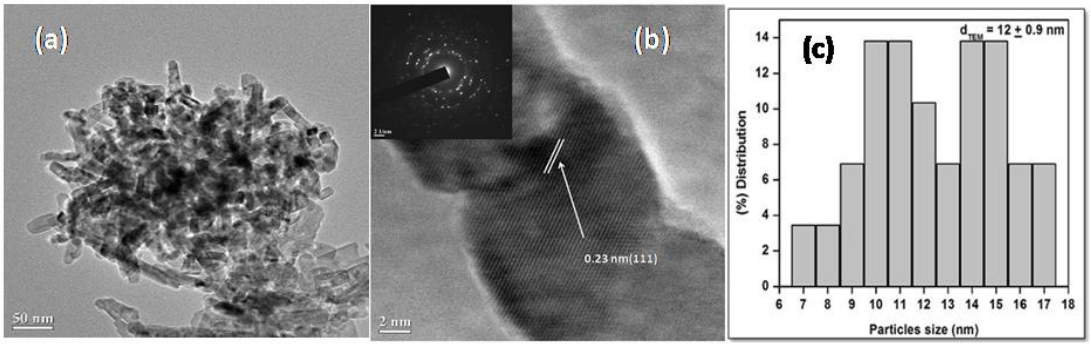

Fig. 7: (a) TEM and (b) HRTEM image of the CuO NPs. Inset in (b) is the SAED pattern of CuO NPs and (c) particle size distribution of the CuO NPs.

4.3.1.8. XPS analysis

The XPS analysis clearly confirmed the presence of Cu^{2+} species in the NPs [Fig. 8(a & b)]. The recycled catalyst contains some hydroxide but, still CuO dominates [Fig. 8(c & d)], i.e. both samples consist mainly of CuO and $Cu(OH)_2$, although recycled catalyst has much higher concentration of $Cu(OH)_2$ than the pristine NPs.

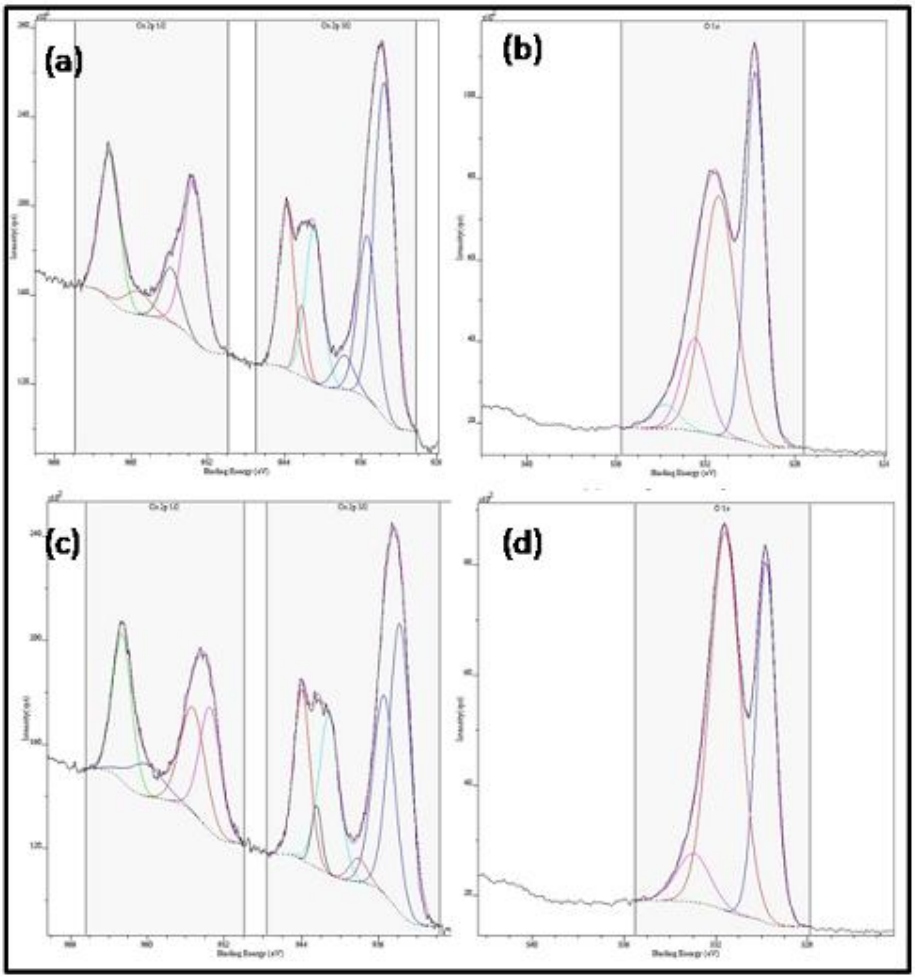

Fig.8: XPS spectra of the catalyst (a & b) and recycled catalyst (c & d).

4.3.2. Optimization of the reaction condition for solvent and base and catalyst

Initially, we started our experiment with the aim to find out the effect of various solvents, bases and amount of catalysts which can effectively catalyzed the reaction between aniline and phenylboronic acid. For this purpose, we have chosen the reaction between phenylboronic acid and aniline as the model reaction and the results are summarized in Table 1.

Initial screening of the effect of different solvents, using K_2CO_3 as base and 15 mol% of the catalyst suggest that MeOH:H_2O (1:1, v/v) was found to be the most efficient solvent system with excellent yields (entry 5, Table 1). After optimizing the solvent system, we studied the effect of the amount of catalyst (entries 5-8, Table 1). From Table 1, it is obvious that 30 mol% of the catalyst with respect to aniline was the optimized amount for the coupling reaction (entry 7, Table 1). With other bases like

Na_2CO_3, Cs_2CO_3, KOH the reaction also proceeds with comparable yields (entries 9-11, Table 1), however, because of the lower molecular weight, cost and lower toxicity of potassium carbonate, it was chosen as the optimized base for the coupling reaction. The controlled reaction conducted under identical conditions devoid of catalyst gave no coupled product despite of prolonged reaction time (entry 12, Table 1). For optimizing the amount of base, we carried the same reaction with 1-2 mmol of the base K_2CO_3 (entries 13 and 14, Table 1) and found that 1.5 mmol is the optimal amount. Again, the presence of an oxidant is critical and an important parameter for the copper promoted *N*-arylation reaction [18]. It has been found that the reaction did not proceed under nitrogen atmosphere (entry 17, Table 1), which confirms the requirement of air as oxidant for the reaction. The air or oxidant in the copper promoted C-N cross-coupling reaction believe to facilitate the oxidation of Cu(II) to Cu(III). The Cu(III), being at higher oxidation state can undergo more facile reductive elimination to form the cross-coupled product compared to Cu(II). Thus, the optimum condition was when the reaction was carried out under air at room temperature in MeOH:H_2O (1:1) solvent system, in the presence of 30 mol% of nanocatalyst with respect to aniline and K_2CO_3 (1.5 mmol) as the base (entry 7, Table 1).

Table 1: Optimization of reaction conditions:[a]

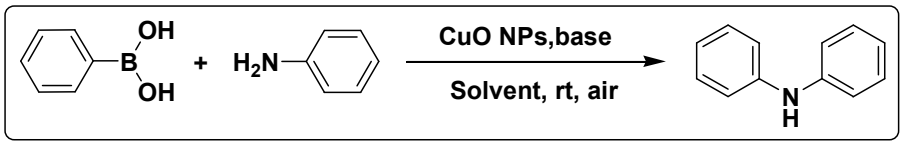

Entry	Solvent	Base	Amount of catalyst (mol %)	Time (h)	Yield(%[b]
1	No solvent	K_2CO_3	15	10	20
2	H_2O	K_2CO_3	15	10	68
3	DCM	K_2CO_3	15	10	54
4	i-PrOH: H_2O(1:1)	K_2CO_3	15	10	58
5	MeOH: H_2O (1:1)	K_2CO_3	15	10	74
6	MeOH: H_2O (1:1)	K_2CO_3	21	10	82
7	MeOH: H_2O (1:1)	K_2CO_3	30	08	92
8	MeOH: H_2O (1:1)	K_2CO_3	36	08	93

9	MeOH: H_2O (1:1)	Na_2CO_3	30	08	86
10	MeOH: H_2O (1:1)	Cs_2CO_3	30	08	88
11	MeOH: H_2O (1:1)	KOH	30	08	66
12	MeOH: H_2O (1:1)	K_2CO_3	-	24	0
13[c]	MeOH: H_2O (1:1)	K_2CO_3	30	08	78
14[d]	MeOH: H_2O (1:1)	K_2CO_3	30	09	92
15[e]	MeOH:H_2O (1:1)	K_2CO_3	30	10	90
16[f]	MeOH:H_2O (1:1)	K_2CO_3	30	10	61
17[g]	MeOH:H_2O (1:1)	K_2CO_3	30	10	0

[a]Reaction Conditions: Phenylboronic acid (1mmol), Aniline (0.5 mmol), K_2CO_3 (1.5 mmol), room temperature stirring. [b]Isolated yield, [c]1mmol of K_2CO_3, [d]2 mmol of K_2CO_3, [e]0.75 mmol Phenylboronic acid used, [f]0.60 mmol Phenylboronic acid used, [g]Nitrogen atmosphere was used.s

We also examined the reaction with different common Cu(II) salts such as $CuSO_4 \cdot 5H_2O$, $Cu(OAc)_2 \cdot H_2O$, CuI and $CuCl_2 \cdot 2H_2O$ for the *N*-arylation reaction of aniline with the optimized reaction condition and found only 15-30% of the product (entries 1-3, Table 2).

Table 2: *N*-Arylation of aniline using different copper(II) salts[a]:

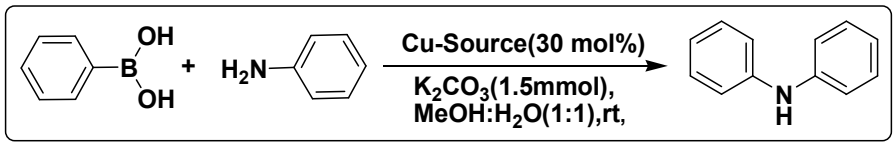

Entry	Cu-source (mol%)	Time (h)	Yield[b] (%)
1	$Cu(OAc)_2 \cdot H_2O$ (10)	24	30
2	$CuSO_4 \cdot 5H_2O$ (10)	24	16
3	$CuCl_2 \cdot 2H_2O$ (10)	24	28
4	CuCl (10)	24	15
5	CuI (10)	24	30
6	CuO NPs (10)	8	92

[a]Reaction conditions: Phenylboronic acid (1 mmol), Aniline (0.5 mmol), K_2CO_3(1.5 mmol), MeOH:H_2O (1:1), room temperature stirring

After optimizing the reaction condition for aniline, our next attempt was to extend the scope of this method for *N*-arylation of imidazole. In this case, we took imidazole (1 mmol) and phenylboronic acid (1.2 mmol) as the model substrates. We found that, here also, the reaction proceeds smoothly only that it requires comparatively longer time than in case of *N*-arylation of aniline and the amount of catalyst required was also found to be 15 mol% with respect to imidazole substrate.

4.3.3. Substrate study

The scope and limitation of the current procedure was evaluated by examining a wide range of electronically diverse anilines and imidazoles with different phenylboronic acid substrates using the prepared CuO NPs. The results are summarized in Table 3.

Table 3: Substrate study

Sl. No	Arylboronic acid	Anilines[a]	Imidazoles[b]	Time (h)	Yield (%)[c]
1	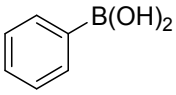	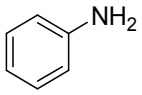	-	8	92
2	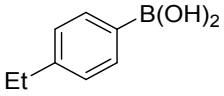	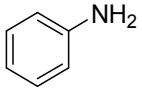	-	8	90
3	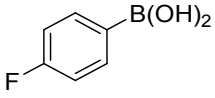	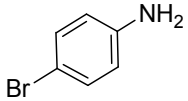	-	10	84
4	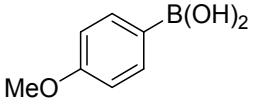	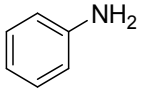	-	8	93
5	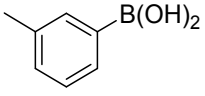	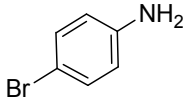	-	10	86
6	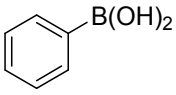	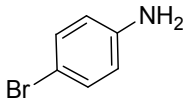	-	9	90
7	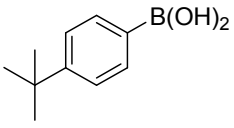	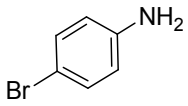	-	8	90

8	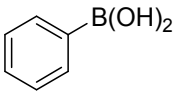	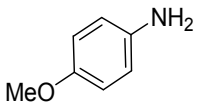	-	8	92
9	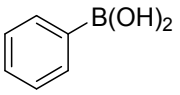	-	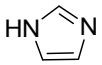	10	88
10	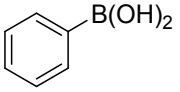	-	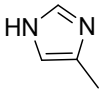	11	84
11	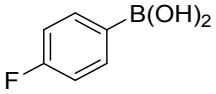	-	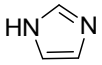	13	81
12	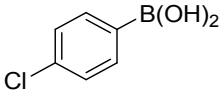	-	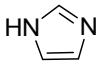	12	86
13	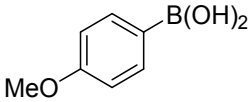	-	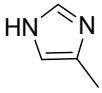	11	86
14	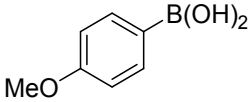	-	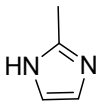	12	82
15	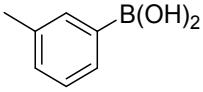	-	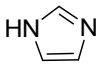	12	82

[a]Reaction conditions: aniline (0.5 mmol), arylboronic acid (1 mmol), nanocatalyst (30 mol% w.r.t. aniline substrate), methanol:water (1:1, v/v) (4 mL), K_2CO_3 (1.5 mmol), rt.

[b]Condition: imidazole (1 mmol), arylboronic acid (1.2 mmol), nanocatalyst (15 mol% w.r.t. imidazole substrate), methanol:water (1:1, v/v) (4 mL), K_2CO_3 (1.5 mmol), rt.

[c]Isolated yield

It was clear from the substrate study that the reaction of arylboronic acids with different aromatics affords good to excellent yields of the cross-coupling products. Anilines having both electron deficient and electron rich groups couple efficiently with boronic acid substrates under the optimized reaction condition resulting excellent yields of the product. However, phenylboronic acid with an electron–donating group couples more efficiently giving better higher yields (entries 4, 7, 13 and 14, Table 3) than those with electron withdrawing groups (entries 3, 11 and 12, Table 3). The compatibility of the

reaction with functional groups likes CN, CO_2R, COR and NO_2 on boronic acid were also examined under the same reaction conditions but the results were not encouraging even after heating (yield less than 25%). The presence of alkyl substituents on the imidazole ring has a little effect in terms of the efficiency of the reaction. For example, 4-methylimidazole takes requires comparatively longer reaction time (entry 10, Table 3) compared to unsubstituted imidazole (entry 9, Table 3).

4.3.4. Reusability study

From the green chemistry point of view, the reusability of the catalysts makes them more attractive. Accordingly, a series of six consecutive runs were carried out using aniline and phenylboronic acid as the model substrate under optimized reaction conditions. For recovery purpose, the scale of the model reaction was increased to two times. After the end of each cycle, the reaction mixture was filtered through Whatmann 40 filter paper and the catalyst was reused for the next batch. From Fig. 9, we find that the catalyst was reusable upto 4^{th} cycle without any significant loss of catalytic activity. It is obvious from Fig. 9 that after 4^{th} cycle, a remarkable loss of catalytic activity occurred. This may be considered due to the deactivation of the catalyst during the course of the reaction and recovery process.

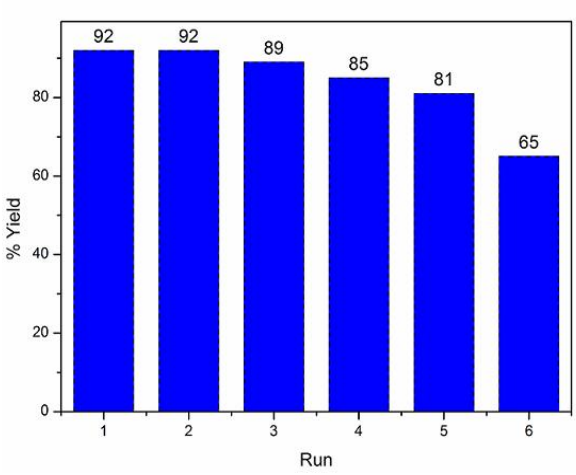

Fig. 9: Reusability of CuO NPs.

4.4. Conclusion

In conclusion, we have developed a very efficient process for the synthesis of CuO NPs, which can effectively catalyzed *N*-arylation of imidazoles and amines under mild

conditions. All the reactions are carried out at room temperature, the procedure works well with a variety of imidazole, aniline and boronic acid substrates having both electron donating and electron withdrawing groups affording good to excellent yields of the product. The catalyst was also found to be reusable upto 4th run without any significant loss of catalytic activity.

Characterization data of the products

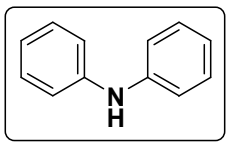

Diphenylamine (entry 1, Table 3): ^{1}H NMR (400 MHz, $CDCl_3$) δ (ppm): 5.71 (b, s, 1H), 6.99 (t, *J*=8Hz, 2H), 7.11-7.13 (m, 4H), 7.30-7.34 (m, 4H). ^{13}C NMR (100 MHz, $CDCl_3$) δ (ppm): 143.2, 129.5, 121.1 and 117.9.

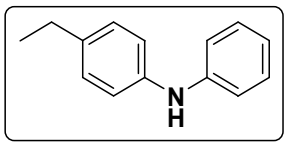

4-Ethyl-*N*-phenylbenzenamine (entry2, Table 3): ^{1}H NMR (400 MHz, $CDCl_3$) δ (ppm): 5.61 (b, s, 1H), 7.23-7.21 (m, 2H), 7.12-7.10 (m, 2H), 7.03-7.00 (m, 4H), 6.87 (t, *J*=8Hz, 1H), 2.59 (q, *J*=8Hz, 3H), 1.24 (m, 2H). ^{13}C NMR (100 MHz, $CDCl_3$) δ (ppm): 143.9, 140.5, 137.5, 129.3, 128.7, 120.4, 118.8, 117.0, 28.2 and 15.8.

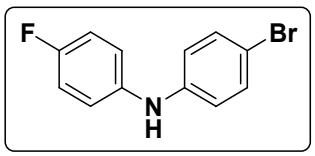

4-Bromo-*N*-(4-fluorophenyl)benzenamine (entry 3, Table 3): ^{1}H NMR (400 MHz, $CDCl_3$) δ (ppm): 5.54 (b, s, 1H), 7.32-7.25 (m, 2H), 7.02-6.96 (m, 4H), 6.82 (d, *J*=8Hz, 2H). ^{13}C NMR (100 MHz, $CDCl_3$) δ (ppm): 143.3, 132.2, 121.3, 121.2, 118.1, 116.2, 116.0 and 112.2.

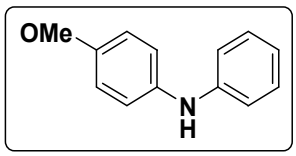

4-Methoxy-*N*-phenylbenzenamine (entries 4 & 8, Table 3): ^{1}H NMR (400 MHz, $CDCl_3$) δ (ppm): 5.49 (b, s, 1H), 7.23-7.16 (m, 3H), 7.08-7.06 (m, 4H), 3.80 (s, 3H). ^{13}C NMR (100 MHz, $CDCl_3$) δ (ppm): 128.2, 128.0, 127.2, 121.1, 118.5, 114.6, 113.6 and 54.5.

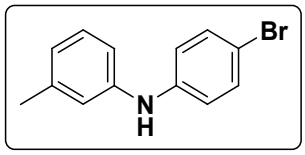

***N*-(4-bromophenyl)-3-methylbenzenamine** (entry 5, Table 3): ^{1}H NMR (400 MHz, $CDCl_3$) δ (ppm): 5.62 (b, s, 1H), 7.33 (d, *J*=8Hz, 2H), 7.16 (t, *J*=8Hz, 1H), 6.92 (d, *J*=8Hz, 2H), 6.86 (m, 2H), 6.78 (d, *J*=8Hz, 1H), 2.30 (s, 3H). ^{13}C NMR (100 MHz, $CDCl_3$) δ (ppm): 142.6, 142.4, 139.4, 132.2, 129.3, 122.6, 119.1, 115.5, 112.5 and 21.5.

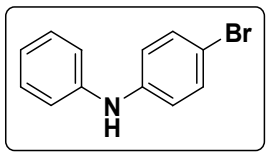

4-Bromo-*N*-phenylbenzenamine (entry 6, Table 3): ^{1}H NMR (400 MHz, $CDCl_3$) δ (ppm): 5.67 (b, s, 1H), 7.35-7.32 (m, 2H), 7.28 (d, *J*=8Hz, 2H), 7.05 (d, *J*=8Hz, 2H), 6.98-6.92 (m, 3H). ^{13}C NMR (100 MHz, $CDCl_3$) δ (ppm): 142.5, 132.2, 129.5, 121.7, 119.1, 118.3 and 112.7

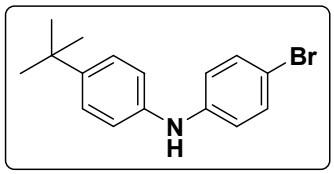

***N*-(4-t-butylphenyl)-4-bromobenzenamine** (entry 7, Table 3): ^{1}H NMR (400 MHz, $CDCl_3$) δ (ppm): 5.64 (b, s, 1H), 7.32-7.29 (m, 4H), 7.01 (d, *J*=8Hz, 2H), 6.89 (d, *J*=8Hz, 2H), 1.31 (s, 9H). ^{13}C NMR (100 MHz, $CDCl_3$) δ (ppm): 139.7, 132.1, 126.2, 118.7, 118.4, 111.9, 34.2 and 30.9.

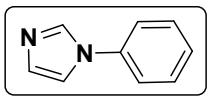

1-Phenyl-1*H*-imidazole (entry 9, Table 3): ^{1}H NMR (400 MHz, $CDCl_3$) δ (ppm): 7.86 (s, 1H), 7.49-7.45 (m, 2H), 7.39-7.34 (m, 3H), 7.27 (m, 1H), 7.19 (s, 1H). ^{13}C NMR (100 MHz, $CDCl_3$) δ (ppm): 137.4, 135.6, 130.3, 129.9, 127.6, 121.6 and 118.3.

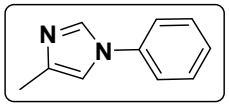

4-methyl-1-phenyl-1*H*-imidazole (entry 10, Table 3): ^{1}H NMR (400 MHz, $CDCl_3$) δ (ppm): 7.75 (s, 1H), 7.49-7.43 (m, 3H), 7.35-7.33 (m, 2H), 7.00 (s, 1H), 2.30 (s, 3H). ^{13}C NMR (100 MHz, $CDCl_3$) δ (ppm): 139.4, 137.5, 134.6, 129.8, 127.2, 125, 6, 121.1, 114.6 and 13.6.

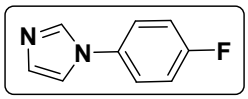

1-(4-fluorophenyl)-1*H*-imidazole (entry 11, Table 3): ^{1}H NMR (400MHz, $CDCl_3$) δ (ppm): 7.80(s, 1H), 7.38-7.35(m, 2H), 7.23-7.18(m, 4H).^{13}C NMR (100MHz, $CDCl_3$) δ(ppm): 162.9, 135.8, 133.6, 130.4, 123.5, 118.6, 116.9, 116.7.

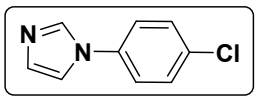

1-(4-chlorophenyl)-1*H*-imidazole (entry 12, Table 3): ^{1}H NMR (400 MHz, $CDCl_3$) δ (ppm): 7.89 (s, 1H), 7.46 (d, *J*=8Hz, 2H), 7.35-7.26 (m, 4H). ^{13}C NMR (100 MHz, $CDCl_3$) δ (ppm): 136.1, 133.3, 120.0 and 122.8.

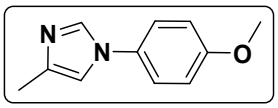

1-(4-methoxyphenyl)-4-methyl-1*H*-imidazole (entry 13, Table 3): ^{1}H NMR (400 MHz, $CDCl_3$) δ (ppm): 7.65 (s, 1H), 7.25 (s, 1H), 7.21 (d, *J*=8Hz, 1H), 6.99-6.92 (m, 3H), 3.83 (s, 3H), 2.28 (s, 3H). ^{13}C NMR (100 MHz, $CDCl_3$) δ (ppm): 158.7, 139.0, 134.8, 130.9, 127.0, 122.9, 114.9, 55.6 and 13.

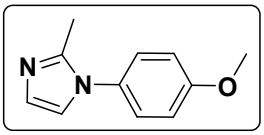

1-(4-methoxyphenyl)-2-methyl-1*H*-imidazole (entry 14, Table 2): ^{1}H NMR (400 MHz, $CDCl_3$) δ (ppm): 3.86 (s, 3H), 2.33 (s, 3H), 7.20 (d, *J*=8Hz, 2H), 7.02-6.95 (m, 4H). ^{13}C NMR (100 MHz, $CDCl_3$) δ (ppm): 159.4, 130.7, 126.9, 121.0, 114.6, 55.6 and 29.7.

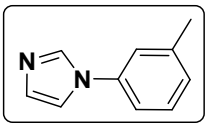

1-*m*-tolyl-1*H*-imidazole (entry 15, Table 3): ^{1}H NMR (400 MHz, $CDCl_3$) δ (ppm): 7.83(s, 1H), 7.34 (t, *J*=8Hz, 1H), 7.26 (s, 1H), 7.18-7.16 (m, 4H), 2.41 (s,3H). ^{13}C NMR (100 MHz, $CDCl_3$) δ (ppm): 140.1, 137.3, 135.6, 130.2, 129.7, 128.2, 122.1, 118.6, 118.3 and 21.4.

^{1}H spectrum of Diphenylamine

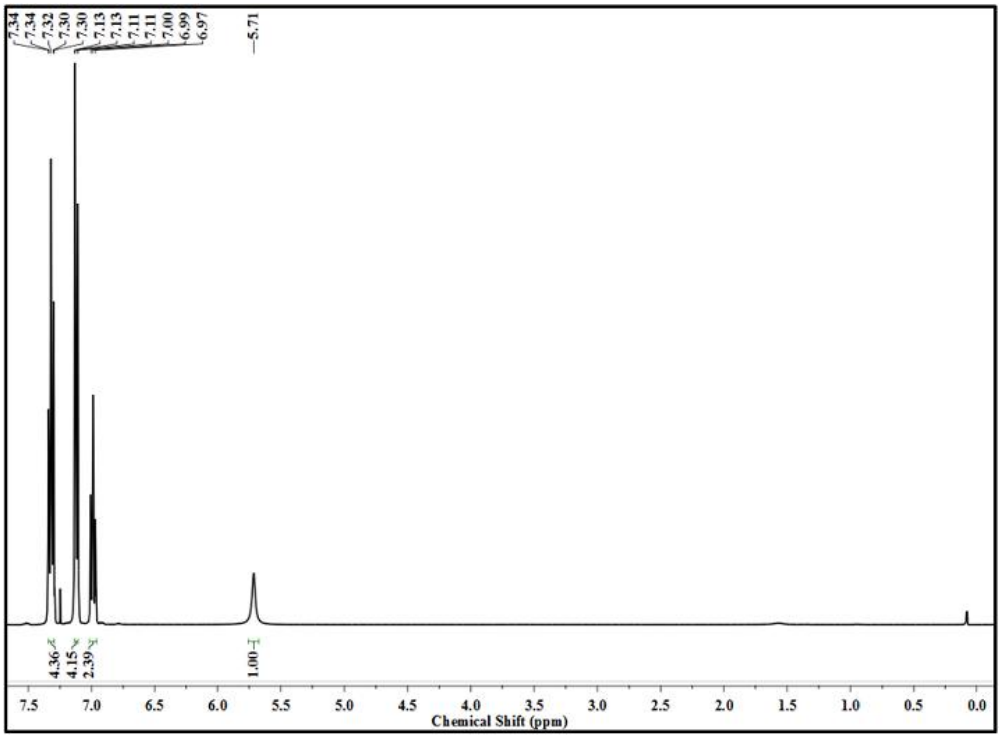

^{13}C NMR spectrum of Diphenylamine

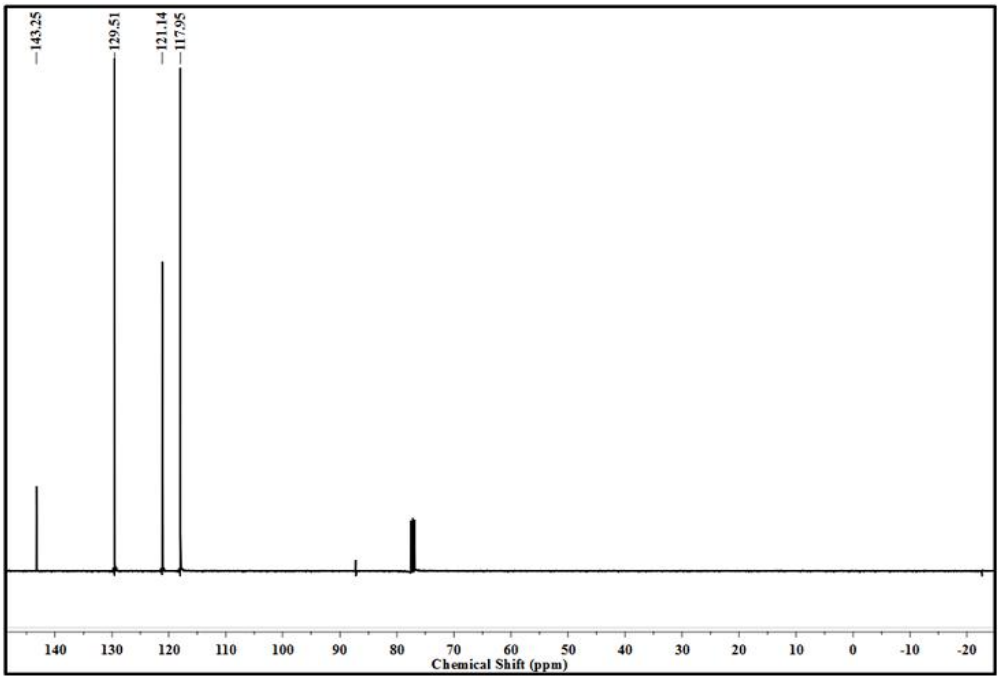

^{1}H NMR spectrum of 1-Phenyl-1*H*-imidazole

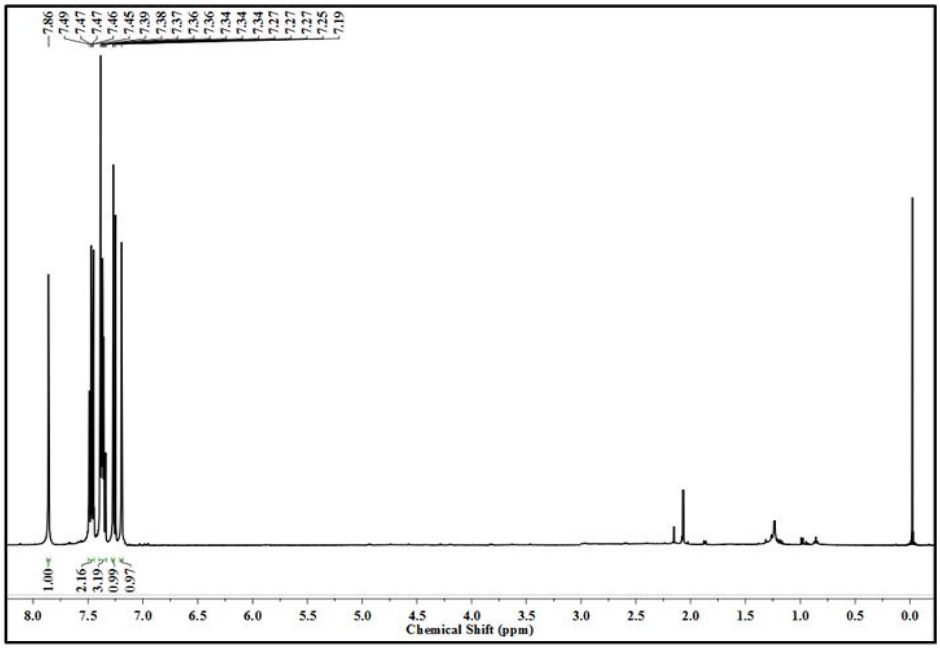

^{13}C NMR spectrum of 1-Phenyl-1*H*-imidazole

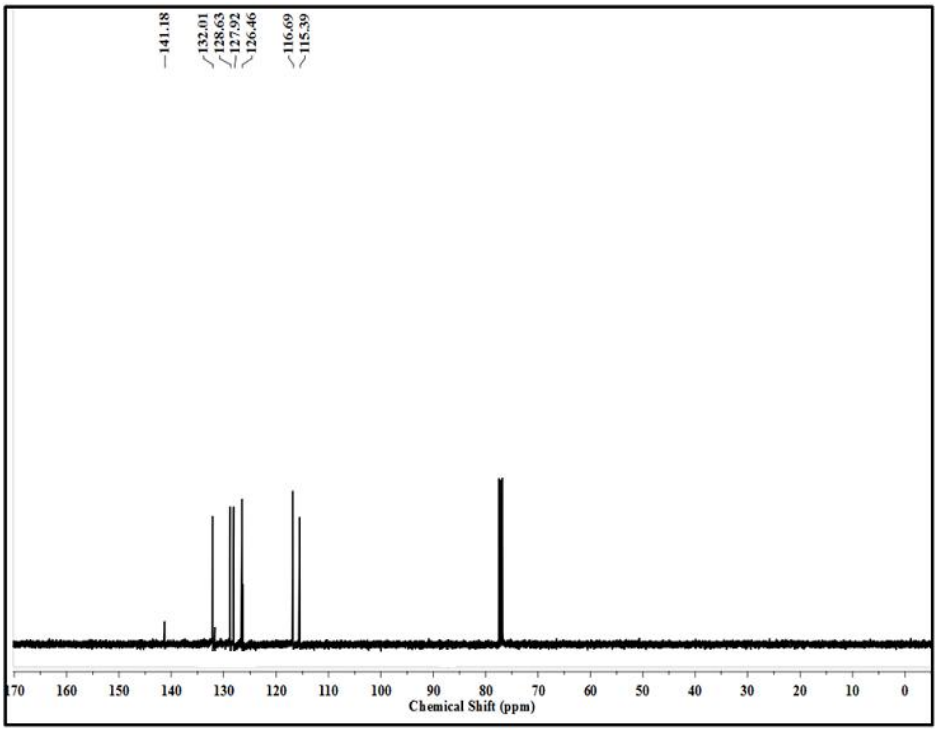

References

[1] (a) Monnier, F. and Taillefer, M. Catalytic C-C, C-N, and C-O Ullmann-Type Coupling Reactions. *Angewandte Chemie International Edition*, 48(38):6954-6971, 2009. (b) Hartwig, J. F Carbon–heteroatom bond formation catalysed by organometallic complexes. *Nature*, 455(7211):314, 2008. (c) Buchwald, S. L Cross coupling. *Accounts of Chemical Research*, 41(11):1439, 2008. (d) Surry, D. S. and Buchwald, S. L. Biarylphosphane ligands in palladium-catalyzed amination. *Angewandte Chemie International Edition*, 47(34):6338-6361, 2008. (e) Evano, G., Blanchard, N., and Toumi, M. Copper-mediated coupling reactions and their applications in natural products and designed biomolecules synthesis. *Chemical Reviews*, 108(8):3054-3131, 2008. (f) Beccalli, E. M., Broggini, G., Martinelli, M., and Sottocornola, S. C−C, C−O, C−N Bond Formation on sp^2 Carbon by Pd (II)-Catalyzed Reactions Involving Oxidant Agents. *Chemical Reviews*, 107(11):5318-5365, 2007. (g) Corbet, J. P. and Mignani, G. Selected patented cross-coupling reaction technologies. *Chemical Reviews*, 106(7):2651-2710, 2006. (h) Beletskaya, I. P. Transition-metal-catalyzed reactions of carbon-heteroatom bond formation by substitution and addition processes. *Pure and Applied Chemistry*, 77(12):2021-2027, 2005.

[2] (a) Iizuka, K., Akahane, K., Momose, D., Nakazawa, M., Tanouchi, T., Kawamura, M., and Iguchi, Y. Highly selective inhibitors of thromboxane synthetase. 1. Imidazole derivatives. *Journal of Medicinal Chemistry*, 24(10):1139-1148, 1981. (b) Wolfe, J. P., Wagaw, S., Marcoux, J. F., and Buchwald, S. L. Rational development of practical catalysts for aromatic carbon−nitrogen bond formation. *Accounts of Chemical Research*, 31(12):805-818, 1998.

[3] (a) Wolfe, J. P., Wagaw, S., Marcoux, J. F., and Buchwald, S. L. Rational development of practical catalysts for aromatic carbon−nitrogen bond formation. *Accounts of Chemical Research*, 31(12):805-818, 1998. (b) Yang, B. H., and Buchwald, S. L. Palladium-catalyzed amination of aryl halides and sulfonates. *Journal of Organometallic Chemistry*, 576(1-2):125-146, 1999.

[4] (a) Lindley, J. copper assisted nucleophilic substitution of aryl halogen. *Tetrahedron*, 40(9):1433-1456, 1984. (b) Paine, A. J. Mechanisms and models for copper mediated nucleophilic aromatic substitution. 2. Single catalytic species from three different oxidation states of copper in an Ullmann synthesis of triarylamines. *Journal of the American Chemical Society*, 109(5):1496-1502, 1987.

[5] Prashad, M., Hu, B., Lu, Y., Draper, R., Har, D., Repic, O., and Blacklock, T. J. β-Hydrogen-containing sodium alkoxides as suitable bases in palladium-catalyzed aminations of aryl halides. *The Journal of Organic Chemistry*, 65(8):2612-2614, 2000.

[6] (a) Chan, D. M. T and Lam, P. Y. S. Recent advances in copper-promoted C-heteroatom bond cross-coupling reaction with boronic acids and derivatives. In Hall, D. G., editor, *Boronic Acids*: *Preparation and Applications in Organic Synthesis and Medicine*, pages. 205-240 Wiley-VCH: Weinheim, 2005. (b) Qiao, J. X. and Lam, P. Y. Copper-promoted carbon-heteroatom bond cross-coupling with boronic acids and derivatives. *Synthesis*, 2011(06):829-856, 2011. (c) Ley, S. V. and Thomas, A. W. Modern synthetic methods for copper-mediated C (aryl)-O, C (aryl)-N, and C (aryl)-S bond formation. *Angewandte Chemie International Edition*, 42(44):5400-5449, 2003. (d) Rao, K. S. and Wu, T. S. Chan–Lam coupling reactions: synthesis of heterocycles. *Tetrahedron*, 38(68):7735-7754, 2012.

[7] Hall, D. G. *Boronic acids: preparation, applications in organic synthesis and medicine*. John Wiley & Sons, 2006.

[8] Lam, P. Y., Vincent, G., Clark, C. G., Deudon, S., and Jadhav, P. K. Copper-catalyzed general C-N and C-O bond cross-coupling with arylboronic acid. *Tetrahedron Letters*, 42(20):3415-3418, 2001.

[9] Antilla, J. C. and Buchwald, S. L. Copper-catalyzed coupling of arylboronic acids and amines. *Organic Letters*, 3(13):2077-2079, 2001.

[10] (a) Rossi, S. A., Shimkin, K. W., Xu, Q., Mori-Quiroz, L. M., and Watson, D. A. Selective formation of secondary amides via the copper-catalyzed cross-coupling of alkylboronic acids with primary amides. *Organic Letters*, 15(9): 2314-2317, 2013. (b) Hügel, H. M., Rix, C. J., and Fleck, K. Comparison of copper (II) acetate promoted N-arylation of 5,5-dimethyl hydantoin and other imides with triarylbismuthanes and aryl boronic acids. *Synlett.*, 2006(14):2290-2292, 2006.

[11] Mondal, M., Sarmah, G., Gogoi, K., and Bora, U. Copper promoted Chan–Lam type *O*-arylation of oximes with arylboronic acids at room temperature. *Tetrahedron Letters*, 53(46):6219-6222, 2012.

[12] Moessner, C. and Bolm, C. $Cu(OAc)_2$-catalyzed *N*-arylations of sulfoximines with aryl boronic acids. *Organic Letters*, 7(13):2667-2669, 2005.

[13] (a) Alonso, F., Moglie, Y., and Radivoy, G. Copper nanoparticles in click chemistry. *Accounts of Chemical Research*, 48(9):2516-2528, 2015. (b) Gawande, M. B., Goswami, A., Felpin, F. X., Asefa, T., Huang, X., Silva, R., and Varma, R. S. Cu and

Cu-based nanoparticles: synthesis and applications in catalysis. *Chemical Reviews*, 116(6):3722-3811, 2016.

[14] (a) Zhang, Q., Zhang, K., Xu, D., Yang, G., Huang, H., Nie, F., and Yang, S. CuO nanostructures: synthesis, characterization, growth mechanisms, fundamental properties, and applications. *Progress in Materials Science*, 60:208-337, 2014. (b) Singh, J., Kaur, G., and Rawat, M. A brief review on synthesis and characterization of copper oxide nanoparticles and its applications. *J. Bioelectron. Nanotechnol*, 1(9):2016.

[15] (a) Gawande, M. B., Goswami, A., Felpin, F. X., Asefa, T., Huang, X., Silva, R., and Varma, R. S. Cu and Cu-based nanoparticles: synthesis and applications in catalysis. *Chemical Reviews*, 116(6):3722-3811, 2016. (b) Lignier, P., Bellabarba, R., and Tooze, R. P. Scalable strategies for the synthesis of well-defined copper metal and oxide nanocrystals. *Chemical Society Reviews*, 41(5):1708-1720, 2012. (c) Wang, L., Cheng, W., Gong, H., Wang, C., Wang, D., Tang, K., and Qian, Y. Facile synthesis of nanocrystalline-assembled bundle-like CuO nanostructure with high rate capacities and enhanced cycling stability as an anode material for lithium-ion batteries. *Journal of Materials Chemistry*, 22(22):11297-11302, 2012.

[16] Goswami, A., Raul, P. K., and Purkait, M. K. Arsenic adsorption using copper (II) oxide nanoparticles. *Chemical Engineering Research and Design*, 90(9):1387-1396, 2012.

[17] Kliche, G. and Popovic, Z. V. Far-infrared spectroscopic investigations on CuO. *Physical Review B*, 42(16):10060, 1990.

[18] (a) Lam, P. Y., Vincent, G., Clark, C. G., Deudon, S., and Jadhav, P. K. Copper-catalyzed general C-N and C-O bond cross-coupling with arylboronic acid. *Tetrahedron Letters*, 42(20):3415-3418, 2001. (b) Lam, P. Y., Clark, C. G., Saubern, S., Adams, J., Averill, K. M., Chan, D. M., and Combs, A. Copper promoted aryl/saturated heterocyclic CN bond cross-coupling with arylboronic acid and arylstannane. *Synlett.*, 2000(05):0674-0676, 2000.